Dubois *et al. EURASIP Journal on Wireless Communications and Networking* 2013, **2013**:260
http://jwcn.eurasipjournals.com/content/2013/1/260

EURASIP Journal on Wireless Communications and Networking
a SpringerOpen Journal

RESEARCH Open Access

Performance of time reversal precoding technique for MISO-OFDM systems

Thierry Dubois[1*], Maryline Hélard[1], Matthieu Crussière[1] and Cécile Germond[2]

Abstract

Time reversal (TR) is considered as a promising technique for green and multi-user communications thanks to its time and space focusing properties. TR can be viewed as a precoding scheme which can be combined with orthogonal frequency division multiplexing (OFDM) and easily carried out in a multiple transmit antenna context. This paper analyzes the performance of TR for a multiple-input single-output (MISO) OFDM system and provides a comparison with maximum ratio transmission (MRT) and equal gain transmission (EGT) precoding techniques. The analytical performance of the three precoding techniques is derived by computing the capacity and the bit error rate (BER) as a function of the transmit signal-to-noise ratio (SNR). First, the capacity analysis highlights the ability of the TR system to provide higher bit rates than the MRT system at low SNRs, while the capacity of the MRT system is the highest at high SNRs. From the obtained BER analytical expressions, the diversity exploitation of each system is discussed. In particular, it is shown that the TR system only exploits half the available diversity, while the systems using EGT or MRT exploit the full diversity. Hence, contrary to what is expected from the theoretical capacity analysis, the TR system is shown to underperform the other precoding schemes in terms of BER. To overcome such a drawback, the combination of TR with classical adaptive modulation techniques is studied, allowing the achievable throughput to be increased without destroying the focusing properties of TR. It is then observed that TR takes advantage of adaptive modulations and outperforms the other schemes at low SNRs. In this study, analytical results and closed-form expressions of capacity and BER performance are provided and confirmed through Monte Carlo simulations.

Keywords: Time reversal; MISO; OFDM; Capacity; Adaptive modulation

1 Introduction

Multiple-antenna communications have raised intense academic and industrial interests in the last two decades and have become a key technology in the evolution of wireless systems (LTE, WLAN, WiMAX, etc.). This success comes from the widely recognized ability of multiple-antenna systems to offer significant improvements in system performance by advantageously exploiting multipath signal propagation to achieve diversity or spatial multiplexing gains [1].

For multiple-input multiple-output (MIMO) systems with available channel state information (CSI) at the transmitter side, techniques based on singular value decomposition (SVD) efficiently exploit spatial diversity [2]. However, the MIMO-SVD approach suffers from the high complexity of the operations required to compute and proceed the precoding and postcoding matrices at the transmitter and receiver sides. Other precoding schemes have thus been introduced, providing suboptimal but simpler solutions to the design of MIMO systems using CSI at the transmitter. In 1999, Lo proposed a precoding system referred to as maximum ratio transmission (MRT) that relies on the matched filter applied at the transmitter side [3]. In 2003, a technique called equal gain transmission (EGT) was introduced, allowing transmission with a unitary gain on every link [4]. In this latter case, precoding only consists of a phase rotation and thus avoids any power imbalance between the signals propagated by each antenna. Considering multiple antennas at the receiver, combining techniques can be carried out in conjunction with a precoding technique to take advantage of the diversity of the signals intercepted by the antenna array.

*Correspondence: thierry.dubois@insa-rennes.fr
[1] Institute of Electronics and Telecommunications of Rennes (IETR), Rennes 35708, France
Full list of author information is available at the end of the article

As far as multiple-input single-output (MISO) systems are concerned, only diversity gain can be expected since the spatial multiplexing gain is driven by the size of the smallest antenna array between transmitter and receiver [5]. For such systems also, since the number of receive antennas $N_r = 1$, postcoding matrices reduce to a scalar value and only precoding operations can be performed. MISO systems are however of high interest considering wireless systems in which receivers cannot afford additional antennas for complexity or size limitation. Considering precoding schemes applied to the MISO context, MRT was demonstrated to reach equivalent performance as SVD under some normalization or scale factor assumptions at the transmitter side [6]. It is also known that EGT and MRT systems exploit full space diversity [4]. These studies have however been led under the assumption of signal propagation over single-band flat fading channels, that is, without taking account any frequency diversity considerations. When considering more wideband transmission systems, diversity exploitation and performance may vary from one precoding scheme to another. In particular, the analysis of MISO precoding schemes applied to waveforms realizing frequency multiplexing such as orthogonal frequency division multiplexing (OFDM) is of high interest.

In that perspective, time reversal (TR) recently appeared as a strong candidate for MISO transmissions because it relies on a simple preprocessing technique for any number of transmit antennas and involves very simple receivers even considering frequency-selective channels. This technique is different from SVD, MRT, or EGT because of the way of weighting the precoding factors over the frequency dimension as it is further detailed in the paper. Moreover, TR benefits from spatial and temporal focusing properties as firstly demonstrated in the ultrasound and underwater acoustics [7] and more recently experimented in wireless communications [8-11]. Pioneer works of Paulraj et al. have namely shown that the richer the scattering environment, the better the time and focusing gains [12]. In UWB systems for instance, TR is suitable as a simple and efficient prefiltering technique for pulse amplitude modulation [13-15] since it is realized over large frequency bandwidths. For systems addressing narrower bandwidths and hereby playing with less rich propagation conditions, the so-called rate back-off or oversampling strategies can be used to compensate for some focusing gain degradation [16,17]. An interesting alternative rather consists in getting the environment richness back from frequency to space by increasing the number of transmit antennas [12]. However, for practical system design where the frequency bandwidth and the size of antenna arrays are limited, imperfect time focusing is likely to be encountered, preventing from a sufficient mitigation of the channel time dispersions. Multicarrier systems such as OFDM are commonly used to deal with time-dispersive channels and can be combined with TR to accommodate any residual intersymbol interference (ISI). The combination of TR and OFDM has recently been studied in [18] and [19] and has been proven to allow designing of simple and efficient MISO-OFDM systems. The fact that TR can be considered as a particular precoding technique of OFDM signals makes it necessary and interesting to be compared with the conventional state-of-the-art MISO-OFDM precoding systems previously mentioned.

In this paper, we propose to lead a complete analysis on the performance of different MISO-OFDM systems based on precoding techniques, including the recently experimented TR approach. Different precoding schemes are analytically studied in terms of capacity and bit error rate (BER) performance. Our conclusions are further confirmed through computer simulations. Even though the differences between the investigated techniques could firstly appear as insignificant, the proposed comprehensive study aims at highlighting the differences between them and demonstrates that their performance varies from system to another. The optimal MRT approach will be considered as benchmark, and all of the other schemes will be analyzed and discussed in terms of performance, capacity, and diversity exploitation. Last but not least, to have a complete view of things, the study will also consider the impact of adaptive modulation strategies applied to the precoded MISO-OFDM systems.

The rest of the paper is organized as follows: In Section 2, the three precoding techniques - MRT, EGT, and TR - are introduced especially when combined with OFDM. In Section 3, the capacity of each system is analytically derived and analyzed. Monte Carlo simulation results are also presented to confirm the theoretical results. In Section 4, the average receive signal-to-noise ratio (SNR) and the average BER of every system are computed, analyzed, and corroborated through Monte Carlo simulations. In Section 5, an adaptive modulation approach is implemented to further improve the performance of every system in terms of achievable throughput. Finally, conclusions are drawn in Section 6.

1.1 Main notations

Vectors and matrices are represented by boldface letters. $\{.\}^*$, $\{.\}^T$, $\{.\}^\dagger$, and Tr{.} are the conjugate, transpose, transconjugate, and trace operators resp. Indices m, n, and k stand for the subcarrier, the time, and the antenna indices resp. For MIMO systems, N_t and N_r stand for the number of transmit and receive antennas resp. For OFDM, N_{FFT} is the number of subcarriers of the system, W_m is the subcarrier bandwidth, and W is the total bandwidth of the system. Symbols $D_{m,n}$, $R_{m,n}$, and $N_{m,n}$ are the transmitted symbol, the received symbol, and the additive

white Gaussian noise (AWGN) sample of power σ_N^2 associated to the mth subcarrier of the nth OFDM symbol resp. Vector $\mathbf{v}_m = \{V_{m,k}\}$ stands for the precoding vector of size N_t applied to the mth subcarrier. Vector $\mathbf{e}_{m,n}$ of size N_t is the transmitted signal vector after precoding. Vector $\mathbf{h}_m = \{H_{m,k}\}$ of size N_t consists of the channel coefficients affecting the mth subcarrier of each spatial link k. Notation λ_m stands for the eigenvalue of $\mathbf{h}_m\mathbf{h}_m^\dagger$. The argument of the channel coefficient $H_{m,k}$ is denoted $\Phi_{H_{m,k}}$. Notations C and C_m are the capacity of the system and of the mth subcarrier resp. The total transmit power is referred to as P_e, and ρ stands for the transmit SNR.

2 Precoding techniques for MISO-OFDM systems

In this section, the precoding techniques that will be compared are introduced. These techniques all require the knowledge of the channel at the transmitter side and are thus suited for closed loop systems. The considered system is a $N_t \times 1$ MISO-OFDM system as depicted in Figure 1 for one subcarrier of index m.

In this figure, $\mathbf{v}_m = \left[V_{m,1}, \ldots, V_{m,k}, \ldots, V_{m,N_t}\right]^T$ represents the precoding function associated to subcarrier m that converts the data symbols $D_{m,n}$ into the transmitted symbols $E_{m,n,k} = D_{m,n}V_{m,k}$, where $V_{m,k}$ is the precoding factor that depends on the antenna index k as well as on the channel response. The channel coefficient on the mth subcarrier for the kth transmit antenna is denoted $H_{m,k}$. We define the channel vector of size N_t as $\mathbf{h}_m = \left[H_{m,1}, \ldots, H_{m,k}, \ldots, H_{m,N_t}\right]$ and the transmitted precoded symbol vector as $\mathbf{e}_{m,n} = \left[E_{m,n,1}, \ldots, E_{m,n,k}, \ldots, E_{m,n,N_t}\right]$.

In our study, the channel is considered as quasi-static which means that it remains constant over several OFDM symbols. For this reason, note that time index n is dropped for channel vector $\mathbf{h}_m$ and precoding vector $\mathbf{v}_m$, but not for symbol vector $\mathbf{e}_{m,n}$.

The symbol received on each subcarrier depends on the applied precoding technique and can thus be expressed as

$$\begin{aligned} R_{m,n} &= \sum_{k=1}^{N_t} H_{m,k}E_{m,n,k} + N_{m,n} \\ &= \sum_{k=1}^{N_t} H_{m,k}V_{m,k}D_{m,n} + N_{m,n} \end{aligned} \quad (1)$$

where $N_{m,n}$ is the AWGN sample associated to the mth subcarrier of the nth OFDM symbol.

The capacity and the average BER expressions of each system will be derived in Sections 3 and 4 resp. In that perspective, the different received signals are firstly expressed in the next paragraphs, highlighting the differences between the applied precoding techniques.

2.1 MRT

For MISO-OFDM systems, the optimal MRT precoding technique is applied to the symbols $D_{m,n}$ to be transmitted using the following precoding factors [20]:

$$V_{m,k} = \frac{H_{m,k}^*}{\sqrt{\lambda_m}} \quad (2)$$

where $\sqrt{\lambda_m} = \sqrt{\sum_{k=1}^{N_t} |H_{m,k}|^2}$ is the singular value of $\mathbf{h}_m$. It should be noted that in this context, MRT is a particular case of SVD with $N_r = 1$.

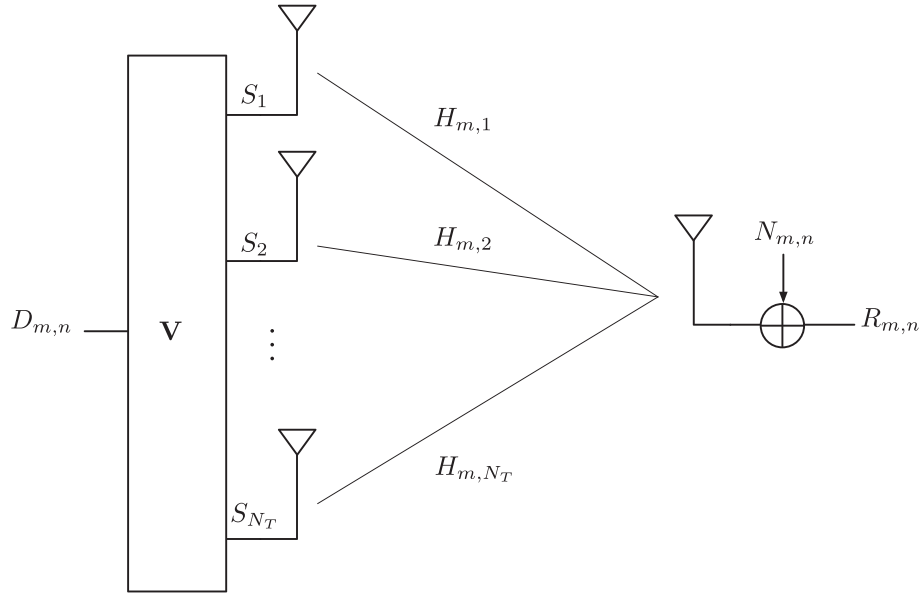

Figure 1 MISO-OFDM system using a precoding technique represented for one subcarrier.

When $H_{m,k}$ follows independent normalized distribution, $E[\lambda_m] = N_t$ and the average power of the transmitted OFDM symbols on each antenna is equal to $1/N_t$. Assuming normalized constellations, total transmit power P_e is then equal to 1. Note however that the instantaneous power associated to each subcarrier depends on instantaneous channel realizations and is not constant across subcarriers.

According to Equations 1 and 2, the received symbol on each subcarrier can finally be expressed as

$$\begin{aligned} R_{m,n} &= \frac{\sum_{k=1}^{N_t} |H_{m,k}|^2}{\sqrt{\lambda_m}} D_{m,n} + N_{m,n} \\ &= \sqrt{\sum_{k=1}^{N_t} |H_{m,k}|^2} D_{m,n} + N_{m,n} \end{aligned} \tag{3}$$

2.2 EGT

Equal gain transmission is derived from MRT and also aims at maximizing the SNR at the receiver side [4]. This technique consists in modifying the phase of the complex symbols before their transmission on every subcarrier of the system.

In the MISO-OFDM context, the precoding vector for EGT is thus [20]

$$V_{m,k} = \frac{e^{j\Phi_{H^*_{m,k}}}}{\sqrt{N_t}} = \frac{e^{-j\Phi_{H_{m,k}}}}{\sqrt{N_t}} \tag{4}$$

where $\Phi_{H^*_{m,k}}$ ($\Phi_{H_{m,k}}$ resp.) is the argument of the channel fading coefficient $H^*_{m,k}$ ($H_{m,k}$ resp.) and $\sqrt{N_t}$ is used for power normalization purpose, that is, to ensure $P_e = 1$. In contrast with the MRT case, the instantaneous power associated to each subcarrier will not vary with the precoding factor since it simply consists of a phase rotation.

According to Equations 1 and 4, the symbol received on each subcarrier is then expressed as

$$\begin{aligned} R_{m,n} &= \sum_{k=1}^{N_t} H_{m,k} \frac{e^{-j\Phi_{H_{m,k}}}}{\sqrt{N_t}} D_{m,n} + N_{m,n} \\ &= \frac{1}{\sqrt{N_t}} \sum_{k=1}^{N_t} |H_{m,k}| D_{m,n} + N_{m,n} \end{aligned} \tag{5}$$

2.3 Time reversal

TR principles are presented in detail for acoustic and electromagnetic waves in [7] and [8] resp. Applied to wireless communications, TR consists in prefiltering the signal with the time reversed and conjugated version of the channel impulse response (CIR) between the transmit and the receive antennas. Without loss of generality, such an operation can be represented in discrete time domain as depicted in Figure 2. In this figure, $g_e[l]$ is the transmit shape filter, $h[l]$ the discrete complex-baseband CIR, $h^*[-l]$ the time reversal filter, and $g[l]$ the so-called equivalent channel obtained by convolving $h[l]$ and $h^*[-l]$.

Consequently, in the time domain, $g[l]$ is made of a central peak of high amplitude and some side lobes. For rich propagation environments, a time focusing effect is obtained as the channel autocorrelation peak is getting sharper and narrower and as side lobes are reduced. In other words, TR leads to time dispersion compression, hereby reducing the ISI occurring between symbols [9]. If time focusing is sufficiently strong for a given symbol duration, the receiver could merely be reduced to a threshold detector. Nevertheless, for systems exploiting a restricted bandwidth or a limited number of transmit antennas, residual ISI can be efficiently treated through multicarrier approach. In contrast with TR which does not modify the symbol structure, OFDM deals with multipath channels by enlarging symbol durations and inserting a guard interval to absorb ISI. When combined with TR, the size of the guard interval is chosen according to the compressed equivalent channel g. Hence, the TR and

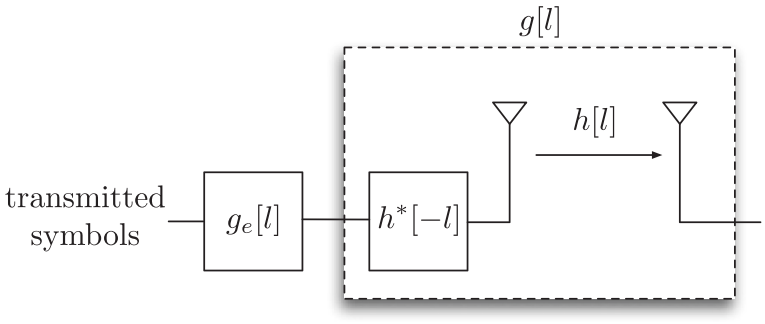

Figure 2 Generic transmission system using time reversal.

multicarrier approaches can be viewed as complementary and compatible processes applied on the signal before transmission, the former trying to compress the channel time dispersions and the latter accommodating with the residual ISI. As already mentioned in the introduction, combination of TR and OFDM is thus of high interest.

In some preliminary work [18], it has been demonstrated that TR can be applied in an OFDM system either in the time or in the frequency domain. For both implementations, the achieved performance is equivalent. In order to keep common notations throughout the paper, we will only consider in the sequel the implementation in the frequency domain.

On that basis, applying TR to an OFDM signal amounts to precoding the symbols on each subcarrier by the conjugated channel coefficients. These channel coefficients are obtained from the frequency version of the CIR through a Fourier transform.

Therefore, the precoding factor is

$$V_{m,k} = \frac{H_{m,k}^*}{\sqrt{N_t}} \tag{6}$$

As in the MRT case, the dependency of the precoding factor to the channel gains leads to instantaneous transmit power variations between the subcarriers. Considering independent normalized processes for the $H_{m,k}$, the total transmit power is however guaranteed to be unitary.

Considering perfect synchronization and a well-dimensioned guard interval, the received symbol after the guard interval removal and after the FFT operation is thus [18]

$$\begin{aligned} R_{m,n} &= \sum_{k=1}^{N_t} H_{m,k} \frac{H_{m,k}^*}{\sqrt{N_t}} D_{m,n} + N_{m,n} \\ &= \frac{1}{\sqrt{N_t}} \sum_{k=1}^{N_t} |H_{m,k}|^2 D_{m,n} + N_{m,n} \end{aligned} \tag{7}$$

2.4 Implementation of the precoding techniques

The choice between these three precoding techniques has to be made considering the multi-antenna array topology. Indeed, the TR and the EGT systems only require the knowledge of the channel for each spatial link independently, i.e., the precoding unit associated to transmit antenna k only needs the knowledge of $H_{m,k}$ for all the subcarriers m but for fixed antenna index k. Such precoding functions can therefore be carried out without any information exchanges between the transmit antennas and are therefore easy to implement in collocated antenna arrays as well as in a fully distributed architecture. Instead, for the MRT precoding, the knowledge of the channel gains for all the spatial links has to be available at each transmit antenna, i.e., each precoding unit has to get the knowledge of $H_{m,k}$ for all the subcarriers m and for all the antennas k. Consequently, MRT is only suitable for antenna arrays for which information exchanges can exist between the antennas, which might result in some constraints of implementation depending on the radio network topology.

In terms of precoding factor computation, TR and MRT might appear as similar at first glance. However, as can be seen in the second column of Table 1, these two techniques are not equivalent. Indeed, the weighting terms of the precoding factor are different, namely $\sqrt{\lambda_m}$ in the MRT case and $\sqrt{N_t}$ in the TR case. The expression of the received signal for the EGT system then differs from the received signal in the TR case by the power of the modulus of the channel coefficients $|H_{m,k}|$. These differences will lead to different SNR expressions at the receiver side and will finally have impact on system performance as studied later on.

As far as computation complexity is concerned, all three precoding techniques require a complex multiplication depending on the channel gains. However, MRT also needs the calculation of the singular values $\sqrt{\lambda_m}$ of the channel on every subcarrier and a complex division by these values. Instead, for TR and EGT, a simple real division by $\sqrt{N_t}$ is needed that can be precomputed in advance since it only depends on the number of transmit antennas. Concerning EGT however, compared to TR, an additional phase computation has to be performed. For easy implementation, such operation can be obtained through a lookup table. Eventually, one can consider that TR and EGT are of comparable complexity, whereas MRT is the most complex.

3 System capacity

In this section, the capacities of the studied systems are derived and compared. Capacity, defined as the maximum

Table 1 Comparison of the main features of MRT-, EGT-, and TR-precoded MISO-OFDM systems

System	Precoding factor	Receive SNR	$\lim_{\rho\to+\infty} \overline{\text{BER}}$	$\overline{\text{BER}}$ for $N_t = 2$	Exploited diversity
MRT	$\frac{H_{m,k}}{\sqrt{\lambda_m}}$	$\left(\sum_{k=1}^{N_t} \lvert H_{m,k}\rvert^2\right)\rho$	$\frac{(2N_t)!}{2^{2N_t+1}(N_t!)^2}\left(\frac{1}{\rho}\right)^{N_t}$	$\frac{3}{16}\frac{1}{\rho^2}$	N_t
EGT	$\frac{e^{\Phi_{H_{m,k}}}}{\sqrt{N_t}}$	$\left(\sum_{k=1}^{N_t} \lvert H_{m,k}\rvert\right)^2 \frac{\rho}{N_t}$	No general closed form	$\frac{1}{4}\frac{1}{\rho^2}$	N_t
TR	$\frac{H_{m,k}}{\sqrt{N_t}}$	$\left(\sum_{k=1}^{N_t} \lvert H_{m,k}\rvert^2\right)^2 \frac{\rho}{N_t}$	$\frac{1}{2^{N_t+1}\left(\frac{N_t}{2}\right)!}\left(\frac{N_t}{\rho}\right)^{\frac{N_t}{2}}$	$\frac{1}{4}\frac{1}{\rho}$	$\frac{N_t}{2}$

achievable throughput for an arbitrary low error probability, is expressed in bit/s and provided for a given transmitted power P_e. In a MISO-OFDM case, the capacity of the mth subcarrier of bandwidth W_m is given as

$$C_m = W_m \log_2\left(1 + \frac{1}{\sigma_N^2}\mathbf{h}_m \Gamma_{e_m} \mathbf{h}_m^\dagger\right) \text{bit/s} \tag{8}$$

where we remind that $\mathbf{h}_m$ contains the related channel fading coefficients for the N_t transmit antennas and with $\Gamma_{e_m} = E\left[\mathbf{e}_{m,n}\mathbf{e}_{m,n}^\dagger\right]$ being the covariance matrix of transmitted signal vector $\mathbf{e}_{m,n}$. The capacity of the whole MISO-OFDM system can be deduced by summing the capacities of all the subcarriers:

$$C = \sum_{m=1}^{N_{\text{FFT}}} C_m = \frac{W}{N_{\text{FFT}}} \sum_{m=1}^{N_{\text{FFT}}} \log_2\left(1 + \frac{1}{\sigma_N^2}\mathbf{h}_m \Gamma_{e_m} \mathbf{h}_m^\dagger\right) \text{bit/s} \tag{9}$$

where W is the total bandwidth of the OFDM signal.

In order to evaluate the capacity of each system whatever the signal bandwidth, we choose to normalize it by the total bandwidth of the signal. It will thus be expressed in bit/s/Hz as

$$\frac{C}{W} = \frac{1}{N_{\text{FFT}}} \sum_{m=1}^{N_{\text{FFT}}} \log_2\left(1 + \frac{1}{\sigma_N^2}\mathbf{h}_m \Gamma_{e_m} \mathbf{h}_m^\dagger\right) \text{bit/s/Hz} \tag{10}$$

Note that the total transmit power of the system is $P_e = \text{Tr}\{\Gamma_{e_m}\}$. In the sequel and in the rest of the paper, the total transmit power is considered as unitary, whatever the system and the number of transmit antennas.

3.1 Capacity of the studied precoding systems

In the case of a precoded signal, the covariance matrix Γ_{e_m} can be calculated as

$$\begin{aligned}\Gamma_{e_m} &= E\left[\mathbf{e}_{m,n}\mathbf{e}_{m,n}^\dagger\right] \\ &= E\left[D_{m,n}D_{m,n}^*\mathbf{v}_m\mathbf{v}_m^\dagger\right] \\ &= P_{e_m}\mathbf{v}_m\mathbf{v}_m^\dagger\end{aligned} \tag{11}$$

where P_{e_m} is the average power allocated on the mth subcarrier before precoding. The capacity can then be deduced as

$$\frac{C}{W} = \frac{1}{N_{\text{FFT}}} \sum_{m=1}^{N_{\text{FFT}}} \log_2\left(1 + \frac{P_{e_m}}{\sigma_N^2}\mathbf{h}_m \mathbf{v}_m \mathbf{v}_m^\dagger \mathbf{h}_m^\dagger\right) \text{bit/s/Hz} \tag{12}$$

In the MISO MRT-OFDM case, the precoding vector is equal to $\mathbf{v}_m = \frac{\mathbf{h}_m^T}{\sqrt{\lambda_m}}$, which yields

$$\left(\frac{C}{W}\right)_{\text{MRT}} = \frac{1}{N_{\text{FFT}}} \sum_{m=1}^{N_{\text{FFT}}} \log_2\left(1 + \frac{P_{e_m}}{\sigma_N^2\lambda_m}\left[\sum_{k=1}^{N_t}|H_{m,k}|^4 + \sum_{i=1}^{N_t}\sum_{\substack{j=1\\ j\neq i}}^{N_t}|H_{i,k}|^2|H_{j,k}|^2\right]\right) \text{bit/s/Hz} \tag{13}$$

In the MISO EGT-OFDM case, the precoding vector is equal to $\mathbf{v}_m = \frac{\Phi_m}{\sqrt{N_t}}$ with $\Phi_m = \left\{e^{-j\Phi_{H_{m,1}}}, \ldots, e^{-j\Phi_{H_{m,k}}}, \ldots, e^{-j\Phi_{H_{m,N_t}}}\right\}$, leading to

$$\left(\frac{C}{W}\right)_{\text{EGT}} = \frac{1}{N_{\text{FFT}}} \sum_{m=1}^{N_{\text{FFT}}} \log_2\left(1 + \frac{P_{e_m}}{\sigma_N^2 N_t}\left[\sum_{k=1}^{N_t}|H_{m,k}|^2 + \sum_{i=1}^{N_t}\sum_{\substack{j=1\\ j\neq i}}^{N_t}|H_{i,k}||H_{j,k}|\right]\right) \text{bit/s/Hz} \tag{14}$$

In the MISO TR-OFDM case, the precoding vector is equal to $\mathbf{v}_m = \frac{\mathbf{h}_m^T}{\sqrt{N_t}}$. We then obtain

$$\left(\frac{C}{W}\right)_{\text{TR}} = \frac{1}{N_{\text{FFT}}} \sum_{m=1}^{N_{\text{FFT}}} \log_2\left(1 + \frac{P_{e_m}}{\sigma_N^2 N_t}\left[\sum_{k=1}^{N_t}|H_{m,k}|^4 + \sum_{i=1}^{N_t}\sum_{\substack{j=1\\ j\neq i}}^{N_t}|H_{i,k}|^2|H_{j,k}|^2\right]\right) \text{bit/s/Hz} \tag{15}$$

3.2 Systems comparison and simulation results

From Equations 13 and 15, it can be noted that the capacities of the MRT and TR systems are very close. They only differ in one weighting term which is $1/\lambda_m$ for the MRT system and $1/N_t$ for the TR system. When the number of antennas increases and the channel fading coefficients are assumed to be independent and to follow a normalized Rayleigh distribution on each subcarrier, λ_m tends towards N_t. As a result, the capacity of the TR system tends towards the capacity of the MRT system as the number of transmit antennas increases without requiring the computation of the singular values $\sqrt{\lambda_m}$. This indicates that TR is thus interesting for systems based on large antenna arrays such as large MIMO systems. On the other hand, the capacity of the EGT system differs from that of

the MRT and the TR systems in the power of the modulus of the channel coefficients within the sum terms.

To corroborate the analytical results, Monte Carlo simulations are carried out. The simulated system is an OFDM system as described above, using either TR, EGT, or MRT as a precoding technique. The channel is supposed to be perfectly known at the transmitter side. Moreover, the modulus of each channel coefficient $H_{m,k}$ is assumed to follow a Rayleigh distribution, independent on each subcarrier and on each antenna, with parameter $\sigma^2 = \frac{1}{2}$. As previously stated, fair performance comparisons are obtained under the assumption of identical transmit power P_e whatever the precoding scheme.

Capacity results are given in Figure 3 for $N_t = 2$, 4, and 16. One can notice that the MRT precoding outperforms the EGT precoding whatever the SNR, with a difference that remains the same whatever the number of transmit antennas. On the other hand, capacity comparisons between TR and the two other schemes depend both on the SNR range and on the number of antennas. The capacity of the TR system is always better or equal to the capacity of the MRT and EGT systems at low SNRs whatever the value of N_t. At high SNRs, the MRT and the EGT systems are the most efficient for a 2×1 system, whereas TR tends to the MRT performance and even outperforms EGT with more than two transmit antennas. Consequently, TR should be preferentially used at a low-SNR regime, while MRT should be more performant at a high-SNR regime. Actually, as expected from the theoretical analysis (see Equations 13 and 15), the difference between the capacity of TR and MRT decreases when the number of transmit antennas increases and both systems become equivalent. This is confirmed with the curves obtained for $N_t = 16$. Recall that this behavior is related to the fact that λ_m tends towards N_t as the number of transmit antennas increases.

From the above observations, it can be understood that TR acts as a power allocation technique that allocates the power on subcarriers experiencing high SNR values. Since TR can be seen as the matched filter on each link between transmit and receive antennas, it works better at low SNRs, outperforming the two other systems. Furthermore, it should be noted that these results do not take into account the spatial focusing property of TR which allows addressing different users while limiting electromagnetic pollution.

4 Bit error rate performance

In this section, the average BER is computed to evaluate the performance of the studied systems. As shown in Section 2, the signal received on each subcarrier for each system depends on the used precoding scheme. Also, it is important to note that due to these precoding functions, the signal entries become statistically dependent on the

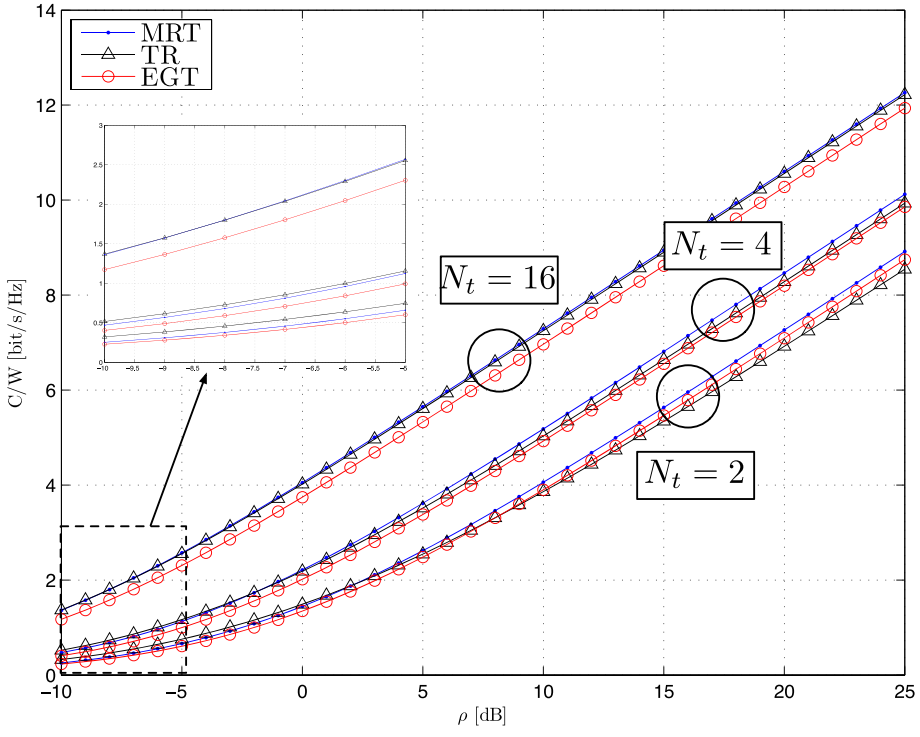

Figure 3 Capacity of MRT-, EGT-, and TR-precoded MISO-OFDM systems for $N_t = 2$, $N_t = 4$, and $N_t = 16$.

channel realizations, hereby affecting the receive power level. We therefore define ρ as the transmit SNR, i.e., the ratio between the total transmit power P_e and the AWGN power σ_N^2, and ρ_{MRT}, ρ_{EGT}, and ρ_{TR} as the receive SNR corresponding to the MRT, EGT, and TR schemes resp. For a same transmit SNR ρ, different receive SNRs will be obtained depending on the used precoding function.

The theoretical performance of each of the presented MISO systems is assessed by computing the average BER for QPSK modulation as a function of transmit SNR ρ. This amounts to comparing the systems at the same transmit power P_e and at the same noise power σ_N^2. For a receive SNR $= x\rho$, where x is a random variable with probability density function (PDF) $p(x)$ that depends on the channel and on the transmit precoding scheme, the average BER is computed as

$$\overline{\mathrm{BER}}(\rho) = \frac{1}{2}\int_{-\infty}^{+\infty} p(x)\cdot \mathrm{erfc}\left(\sqrt{x\rho}\right) dx \tag{16}$$

4.1 MISO-MRT-OFDM system

The receive SNR for such a transmission, denoted ρ_{MRT}, can be derived from Equation 3 as

$$\rho_{\mathrm{MRT}} = \frac{\left(\sqrt{\sum_{k=1}^{N_t}|H_{m,k}|^2}\right)^2 P_e}{\sigma_N^2} = \left(\sum_{k=0}^{N_t}|H_{m,k}|^2\right)\rho = x\rho \tag{17}$$

The BER is then computed using Equation 16 with $x = \sum_{k=1}^{N_t}|H_{m,k}|^2$. Given the assumptions on $|H_{m,k}|$, x is a sum of independent identically distributed Gaussian variables with standard deviation $\sigma = \frac{1}{\sqrt{2}}$. It can be deduced that x follows a Gamma distribution with a shape parameter of N_t and a scale parameter of $2\sigma^2 = 1$. Hence,

$$p(x) = \begin{cases} \frac{1}{\Gamma(N_t)} x^{N_t-1}e^{-x} & \text{for } x > 0 \\ 0 & \text{else} \end{cases} \tag{18}$$

where $\Gamma(.)$ is the Gamma function.

After integrating Equation 18 in Equation 16 and leading the computation (see Appendix 1, the BER expression becomes

$$\overline{\mathrm{BER}}_{\mathrm{MRT}}(\rho) = \frac{1}{\Gamma(N_t)}\sum_{k=0}^{+\infty}\frac{(-1)^k}{k!}\left(\frac{1}{\rho}\right)^{k+N_t}\frac{\Gamma\left(k+N_t+\frac{1}{2}\right)}{2\sqrt{\pi}(k+N_t)} \tag{19}$$

If the transmit SNR ρ tends towards infinity, the asymptotic average BER can be computed as the term containing the highest power of ρ:

$$\lim_{\rho\to+\infty}\overline{\mathrm{BER}}_{\mathrm{MRT}}(\rho) = \frac{(2N_t)!}{2^{2N_t+1}(N_t!)^2}\left(\frac{1}{\rho}\right)^{N_t} \tag{20}$$

4.2 MISO-EGT-OFDM system

In the EGT case now, the receive SNR ρ_{EGT} obtained from Equation 5 can be expressed as

$$\rho_{\mathrm{EGT}} = \left(\sum_{k=1}^{N_t}|H_{m,k}|\right)^2\frac{\rho}{N_t} = y^2\frac{\rho}{N_t} \tag{21}$$

It follows that the average BER can be computed as

$$\overline{\mathrm{BER}}_{\mathrm{EGT}}(\rho) = \frac{1}{2}\int_{-\infty}^{+\infty} p(y).\mathrm{erfc}\left(y\sqrt{\frac{\rho}{N_t}}\right) dy \tag{22}$$

with $y = \sum_{k=1}^{N_t}|H_{m,k}|$. The PDF of y is a sum of random variables following a Rayleigh distribution. No closed form can be found in the literature for any N_t, but some approximations exist. In the following, we propose to derive the exact computation for $N_t = 2$. In Appendix 2, the PDF of y is proven to be

$$p(y) = \frac{e^{-\frac{y^2}{4\sigma^2}}}{\sigma^3}\left\{\sqrt{\pi}erf\left(\frac{y}{2\sigma}\right)\left(\frac{y^2}{4}-\frac{\sigma^2}{2}\right)+\frac{y\sigma}{2}e^{-\frac{y^2}{4\sigma^2}}\right\} \tag{23}$$

yielding the following closed-form expression of the BER (see Appendix 2 for further details):

$$\begin{aligned}\overline{\mathrm{BER}}_{\mathrm{EGT}}(\rho) =& \frac{1}{4\sigma^3}\sum_{k=0}^{+\infty}\sum_{l=0}^{+\infty}\frac{(-1)^{k+l}}{k!\,l!\,(2l+1)2^{2k+2l+1}\sigma^{2k+2l+1}} \\ &\times\left\{\left(\frac{2}{\rho}\right)^{k+l+2}\frac{\Gamma\left(k+l+\frac{5}{2}\right)}{2\sqrt{\pi}(k+l+2)}\right. \\ &\left.-2\sigma^2\left(\frac{2}{\rho}\right)^{k+l+1}\frac{\Gamma\left(k+l+\frac{3}{2}\right)}{2\sqrt{\pi}(k+l+1)}\right\} \\ &+\frac{1}{4\sigma^2}\sum_{k=0}^{+\infty}\frac{(-1)^k}{k!\,2^k\sigma^{2k}}\left(\frac{2}{\rho}\right)^{k+1}\frac{\Gamma\left(k+\frac{3}{2}\right)}{2\sqrt{\pi}(k+1)}\end{aligned} \tag{24}$$

At high SNR, it is also demonstrated in Appendix 2 that

$$\lim_{\rho\to+\infty}\overline{\mathrm{BER}}_{\mathrm{EGT}}(\rho) = \frac{1}{16\sigma^4}\frac{1}{\rho^2} = \frac{1}{4}\frac{1}{\rho^2} \tag{25}$$

For a higher number of transmit antennas, the exact computation of the average BER becomes no more tractable, and only approximated expressions could be obtained. In this paper, we then choose to extend the results through simulation results as detailed in Section 4.4.

4.3 MISO-TR-OFDM system

Concerning the MISO-TR-OFDM system, the receive SNR ρ_{TR} is first computed based on the received signal Equation 7:

$$\rho_{\mathrm{TR}} = \left(\sum_{k=1}^{N_t} \frac{|H_{m,k}|^2}{\sqrt{N_t}}\right)^2 \frac{P_e}{\sigma_N^2} = \left(\sum_{k=1}^{N_t} |H_{m,k}|^2\right)^2 \frac{\rho}{N_t} = x^2 \frac{\rho}{N_t} \tag{26}$$

The average BER is obtained according to Equation 22 while substituting y by $x = \sum_{k=1}^{N_t} |H_{m,k}|^2$. The PDF of x is thus the same as in Section 4.1 and follows a Gamma distribution (see Equation 18). After a development in Taylor series of this expression and a variable change (see Appendix 3, one gets

$$\overline{\mathrm{BER}}_{\mathrm{TR}}(\rho) = \frac{1}{2\Gamma(N_t)} \sum_{k=0}^{+\infty} \frac{(-1)^k}{k!} \frac{\Gamma\left(\frac{k+N_t+1}{2}\right)}{2\sqrt{\pi}\left(\frac{k+N_t}{2}\right)} \left(\sqrt{\frac{N_t}{\rho}}\right)^{k+N_t} \tag{27}$$

At high SNR, we finally have

$$\lim_{\rho \to +\infty} \overline{\mathrm{BER}}_{\mathrm{TR}}(\rho) = \frac{1}{2^{N_t+1}\left(\frac{N_t}{2}\right)!} \left(\frac{N_t}{\rho}\right)^{\frac{N_t}{2}} \tag{28}$$

4.4 System comparison and simulation results

The analytical expressions previously obtained for the receive SNR and the asymptotic BER for any number of transmit antennas are summarized in Table 1. In addition, the last two columns provide the asymptotic BER for $N_t = 2$ and the deduced exploited diversity order for each system whatever N_t. Such a diversity order is evaluated by determining the power factor of ρ in the asymptotic average BER expressions. As previously explained, no general closed form exists for the asymptotic BER for the EGT system. The expected diversity to be exploited is therefore given by extension from the result obtained for $N_t = 2$ and is confirmed hereafter by the simulation results. From this table, many differences have to be highlighted in terms of exploited diversity and SNR gain at high-SNR extreme.

At first, the systems using the MRT and the EGT precoding schemes are expected to exploit the full diversity N_t for any number of transmit antennas, while the system using TR only exploits half the available diversity. Such difference is due to the factors affecting the receive SNR and to their statistical properties. For TR indeed, the factor is a squared sum of the squared modulus of the channel coefficients. By developing this squared sum, some channel coefficients appear with a power equal to 4, whereas in the case of the MRT and EGT, the terms appear with a power equal to 2. After the analytical developments detailed in the previous sections and Appendices, the obtained BER expressions exhibit a power term of N_t for the MRT precoding and $N_t/2$ for the TR one.

In addition to the considerations on the exploited diversity, it is interesting to focus on the receive SNR gains observed at high-SNR regime. From the asymptotic BER obtained for $N_t = 2$, MRT obviously outperforms EGT because of the weighting factor of the $1/\rho^2$ term, i.e., 3/16 instead of 1/4. Moreover, the TR asymptotic BER being equal to $\frac{1}{4\rho}$, TR neither benefits from a diversity gain nor from an SNR gain compared to the other schemes.

Monte Carlo simulations have been carried out to confirm the analytical results and to extend the previous analytical results whatever the number of transmit antennas. The simulated system is the same as described in Section 3.2. Once again, one has to keep in mind that fair performance comparisons are obtained under the assumption of identical transmit power and unchanged noise level whatever the precoding scheme. On that basis, BER curves are plotted versus E_b/N_0 directly derived from transmit SNR ρ, i.e., $(E_b/N_0)_{\mathrm{dB}} = \rho_{\mathrm{dB}} - 3$ dB for QPSK modulation. Note also that BER results are all obtained keeping the same guard interval size for the three studied precoding systems.

It can be observed in Figures 4 and 5 that the asymptotic slopes summed up in Table 1 perfectly match the average BER curves. More precisely, in Figure 4, for the 2×1 system, the average BER of the TR system decreases as -10 dB/decade, which indicates an exploited diversity of 1 (div 1 in the figure), whereas the slope for the EGT and the MRT systems is -5 dB/decade, revealing an exploited diversity of 2 (div 2 in the figure). The same observations can be made in Figure 5 for $N_t = 4$, where the MRT and the EGT systems both exploit a diversity order equal to 4 (slope of -2.5 dB/decade) and the TR system exploits a diversity order of 2. In addition, note that the MRT system slightly outperforms the EGT system which corresponds to the SNR gain previously discussed. EGT therefore approaches the best BER performance, while keeping a lower complexity as already indicated in Section 2.4. These observations corroborate the theoretical results obtained for the MRT and the TR systems on the exploited diversity for a $N_t \times 1$ system and allow extending the results obtained for $N_t = 2$ for the EGT system. A fundamental conclusion is then that the systems using MRT or EGT exploit the full diversity N_t, while the system using TR only exploit half of the diversity, i.e., $N_t/2$.

Nevertheless, it has been shown in Section 3 that the capacity of the system using TR is higher than the capacity of the EGT system for $N_t > 2$ and very close to the capacity of the MRT system. Hence, in terms of BER, the TR system does not perform as good as expected from capacity considerations. Indeed, the system would theoretically need an SNR of about 3 dB (resp. -1dB) to achieve

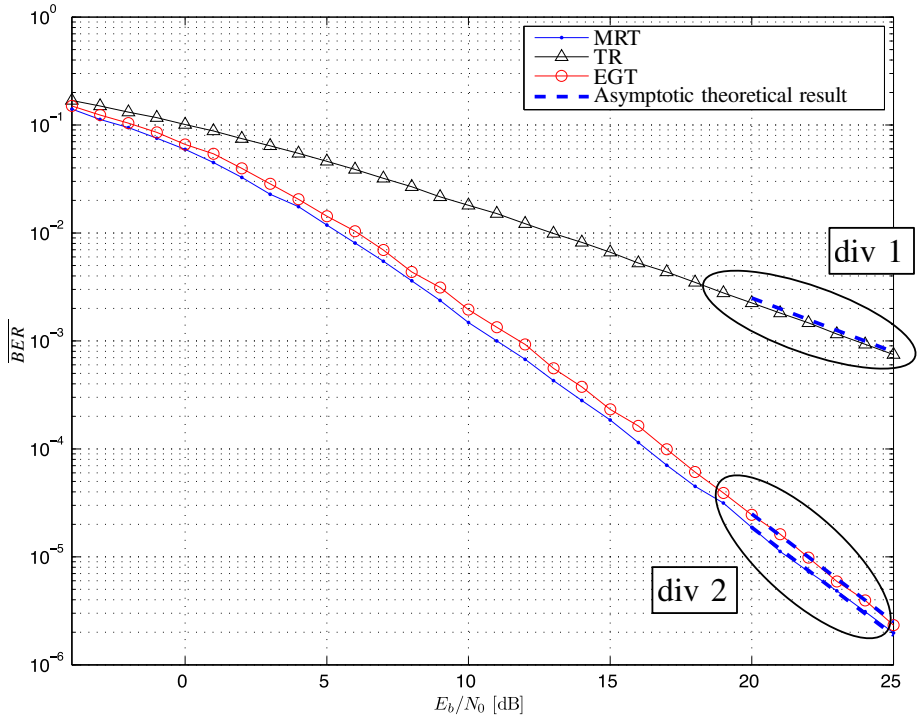

Figure 4 BER performance of MRT-, EGT-, and TR-precoded MISO-OFDM systems for $N_t = 2$.

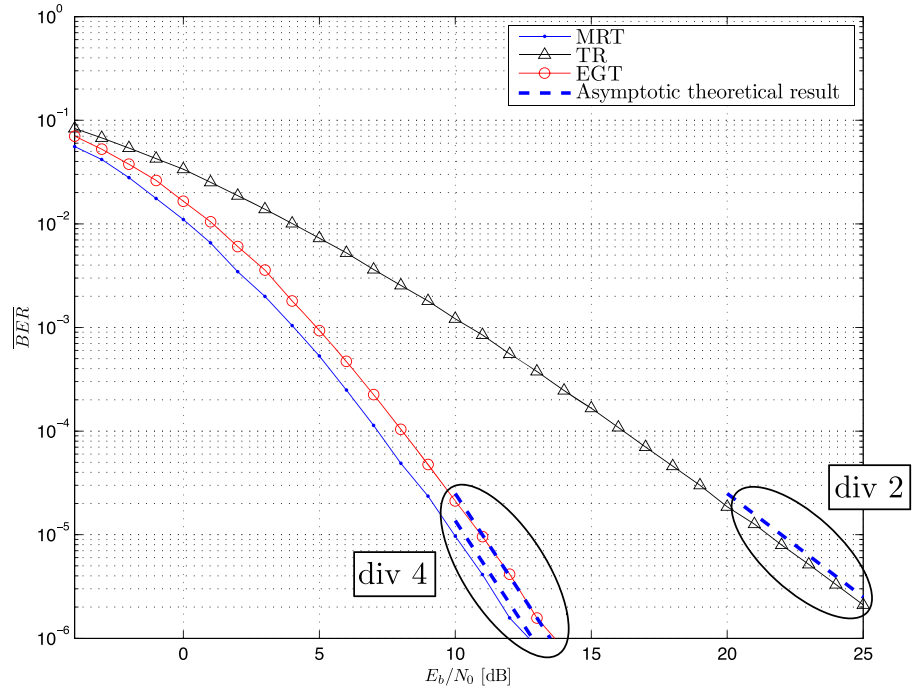

Figure 5 BER performance of MRT-, EGT-, and TR-precoded MISO-OFDM systems for $N_t = 4$.

a spectral efficiency of 2 bit/s/Hz for $N_t = 2$ ($N_t = 4$ resp.). However, using the asymptotic expression for the average BER with QPSK modulation, i.e., at 2 bit/s/Hz (see Table 1), the necessary SNR value to achieve a BER of 10^{-5} with a TR system is equal to 44 dB for $N_t = 2$ and 22 dB for $N_t = 4$. Hence, the system should theoretically be able to operate at a better rate. On this basis, we propose to study adaptive modulations in the next section.

5 Adaptive modulation

The fact that the TR system underperforms the other schemes in terms of BER can be interpreted as being due to the use of constant order modulation across the subcarriers of the OFDM system. As evident from Equations 3, 5, and 7, in the TR system, the QPSK symbols experience equivalent channel gains with components proportional to $|H_{m,k}|^2$ instead of $|H_{m,k}|$ for the MRT and the EGT schemes. This means that for the subcarriers associated to high $|H_{m,k}|$ values, TR could probably use modulations of higher order compared to the other schemes. For this reason, we propose to study the impact of the use of adaptive modulations.

More generally, a conventional solution to get closer to the capacity when having CSI knowledge at the transmitter consists in applying a power allocation algorithm per subcarrier or per antenna. However, the EGT technique, by definition, should not be combined with a power allocation technique as it supposes to have a unity gain on each subcarrier. On the other hand, as the main advantage of TR is its time and spatial focusing properties, combining it with a power allocation algorithm would be equivalent to changing the shape of the filter, hereby destroying the TR focusing effects. The MRT system could benefit from a power allocation algorithm, but for fair comparison purpose, it will not be done here.

To approach capacity, a bit allocation algorithm can alternatively be carried out, leading to adaptive modulation strategies [21]. It will allow the three systems to transmit symbols of higher order on subcarriers with a better SNR to ensure a target symbol error rate (SER).

The capacity being calculated for a close to zero BER, a target SER must be set to take into account the performance of the QAM modulations. We choose here to set it to 10^{-5}. Knowing the SNR required for different QAM modulations to achieve a SER equal to 10^{-5} on a Gaussian channel allows us to determine which order of modulation should be used on each subcarrier according to the related SNR. As shown in Section 4, such SNR values also depend on the precoding technique carried out in the system, which means that the orders of the constellations will strongly vary from one technique to another. Actually, the maximum throughput that can be achieved on a given flat-fading channel can be expressed as [21]

$$R = \log_2\left(1 + \frac{1}{\rho_0}\frac{P_s}{\sigma_N^2}\right) \tag{29}$$

where P_s is the power of the transmitted signal and parameter ρ_0 is commonly called the 'normalized SNR'. It is expressed as

$$\rho_0 = \frac{\mathrm{SNR}}{2^R - 1} \tag{30}$$

where R is the number of bits per symbol. ρ_0 represents the SNR gap between the channel capacity and the SER operating point of the QAM modulations with Gray code. This gap turns out to be constant whatever the number of states of the modulation and can easily be obtained from the SER expression as follows [21]:

$$\mathrm{SER} \approx 2\mathrm{erfc}\left(\frac{3R}{2(2^R - 1)}\frac{E_b}{N_0}\right) \tag{31}$$

Using Equations 30 and 31 and knowing that $E_s/N_0 = RE_b/N_0$, it becomes

$$\mathrm{SER} \approx 2\mathrm{erfc}\left(\frac{3}{2}\rho_0\right) \tag{32}$$

For instance, a target SER of 10^{-5} leads to a gap value of $\rho_0 = 6.94$, i.e., 8.4 dB. Note that this gap value could be updated considering a system using channel coding without changing the principle of the bit loading approach. In such a case, the allocation process would simply select appropriate modulation/coding couples to respect the target SER.

Following this approach, it is possible to compute the achieved throughput for any of the studied precoding techniques, as proposed in Figure 6 for $N_t = 2$. The capacity curve obtained for each of the systems is also drawn in this figure as a reference. One can notice that the hierarchy of the curves obtained for the achieved throughputs remains the same as that obtained when considering capacity results.

For $N_t = 2$, the TR system achieves a spectral efficiency of 2 bit/s/Hz with a SER of 10^{-5} at a SNR of 13 dB, against more than 40 dB when only QPSK is used without any adaptive modulation. Consequently, owing to adaptive modulation, the three systems perform very close to each other at 2 bit/s/Hz. Moreover, we observe that the system offering the best throughput up to a SNR of 11 dB is the TR system. As expected for SNR values greater than 11 dB, the system offering the best throughput is the MRT system. This means that at low SNR, the TR-based system is capable of assigning a higher average number of bits to the subcarriers. Meanwhile, based on the capacity results obtained in Figure 3, the TR scheme is expected to reach

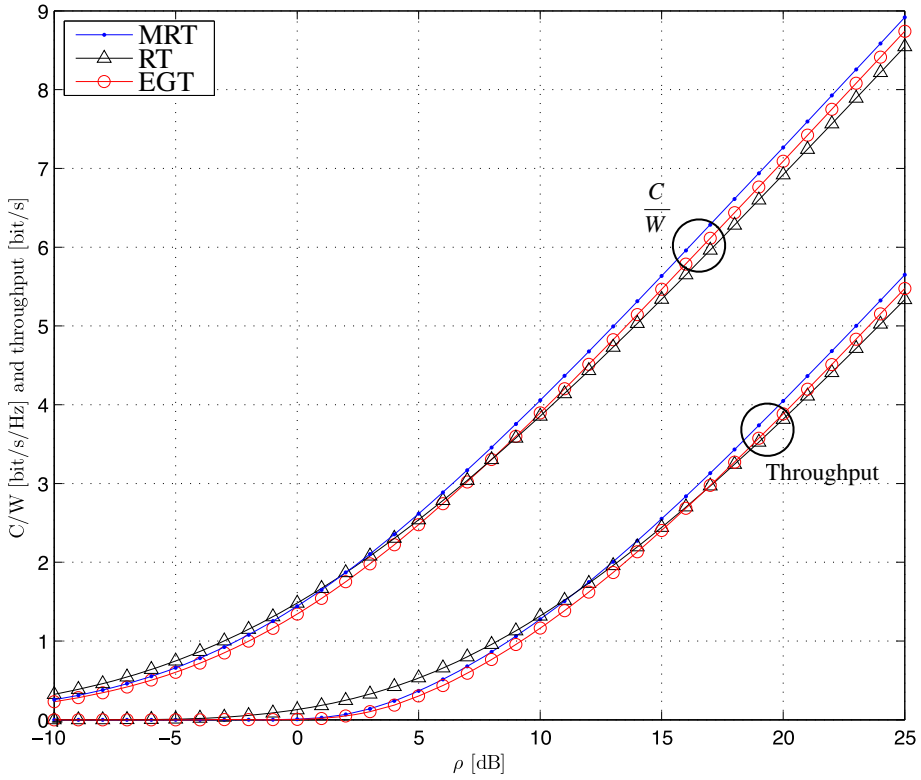

Figure 6 Capacity and achievable throughput of MRT-, EGT-, and TR-precoded MISO-OFDM systems for target SER $= 10^{-5}$ and $N_t = 2$.

the performance of the MRT scheme at high SNR for a greater number of transmit antennas.

Complementary to throughput results, Figure 7 gives the distribution of the number of states assigned to the subcarriers for a SNR equal to 0 dB. In this figure, value 0 on the x-axis means that no symbol is sent on the subcarriers. Value 2^M means that 2^M-QAM symbols are allocated to the subcarriers. It can be noticed that the TR system allocates symbols from the BPSK (1 bit per symbol) up to the 16-QAM modulation (4 bits per symbol), whereas the other systems only transmit BPSK symbols and this for a very small number of subcarriers. This reveals that the receive SNR of some subcarriers is better when using TR than using MRT or EGT. The same kind of distributions can be obtained for a SNR of 25 dB and are given in Figure 8. It can be observed that the TR system range of the used constellation orders is higher than that obtained for the two other systems. More precisely, the TR system allocates 1,024-QAM symbols while the other systems only go up to 512-QAM. This reveals again that some subcarriers experience a better receive SNR in the TR system. On the other hand, the fact that the TR system allocates more BPSK and QPSK symbols reveals that more subcarriers experience a low SNR in the TR system than the two other systems. As mentioned in the beginning of this section, this has to be related to the fact that modulation symbols experience different equivalent channel gains. As the equivalent channel for the TR system can be viewed as more frequency selective, adaptive modulations lead to the use of a wider range of constellation orders than the other studied systems. Nevertheless, throughput results obtained in Figure 6 show that the three systems tend to perform similarly as the transmit SNR level increases.This can be understood by the fact that the subcarriers experiencing high channel gains compensate the other subcarriers for their low channel gains, hereby leading to equivalent average throughput.

6 Conclusion

In this paper, different precoding techniques for a MISO-OFDM system have been studied: time reversal, maximum ratio transmission, and equal gain transmission techniques. It has been highlighted that depending on the precoding schemes, the transmitted signal experiences different equivalent channels, therefore leading to fundamental differences in terms of capacity, SNR gain, and diversity exploitation capability. All the results have been derived through analytical studies and confirmed or extended through simulations. Eventually, the three considered precoding techniques may appear quite similar at first look, but the choice between these three techniques

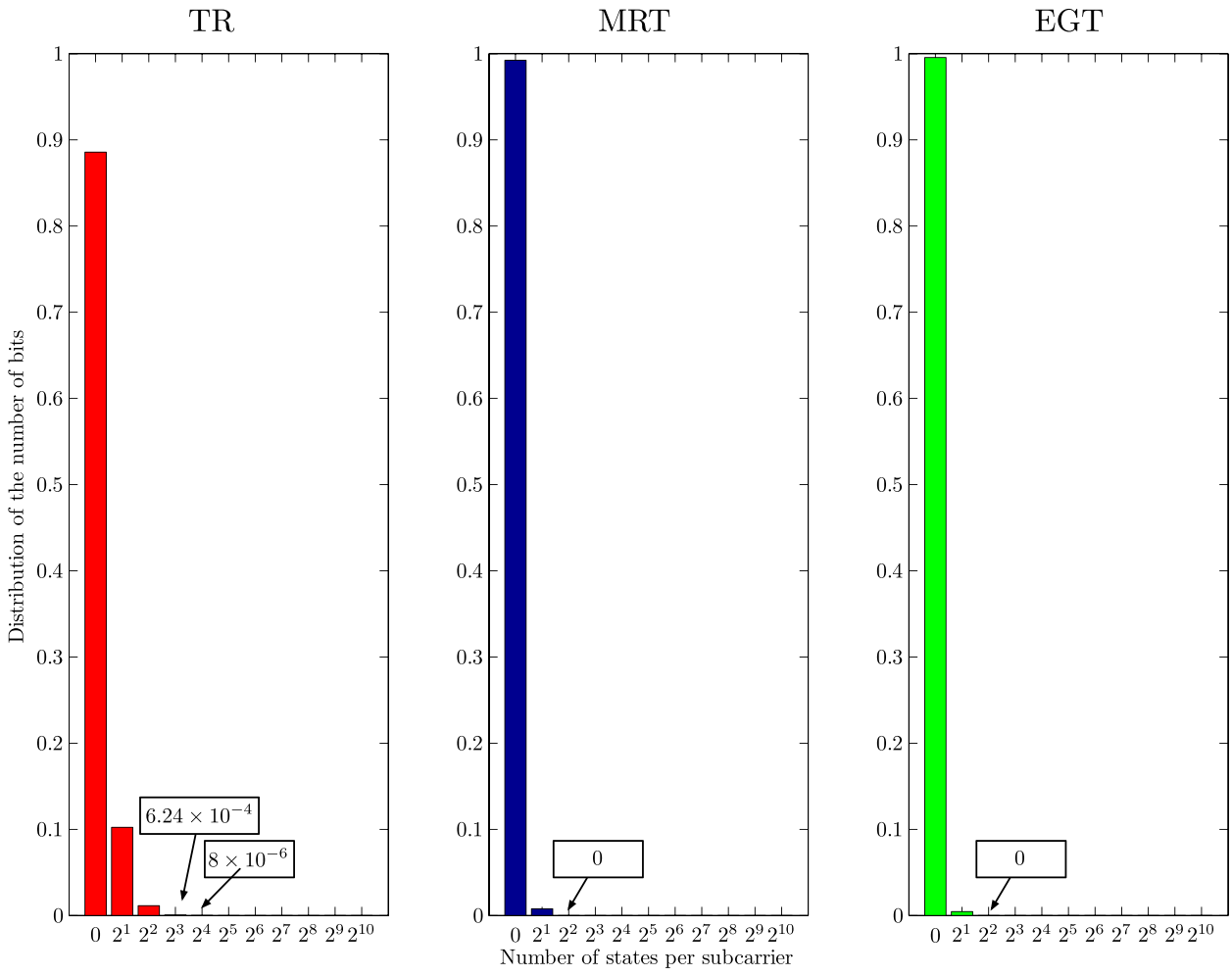

Figure 7 Distribution of number of bits allocated on subcarriers for transmit SNR $\rho = 0$ dB, $N_t = 2$ and target SER of 10^{-5}.

must be made considering the size and the topology of the transmit antenna array, the SNR range, and the eventual use of adaptive modulations.

As far as capacity is concerned, it has been shown that the TR system performs the best at low SNRs, whereas the capacity of the MRT system is the best at high SNRs, even if the TR and the MRT systems interestingly become equivalent when the number of transmit antennas increases.

In terms of BER, however, the MISO-OFDM systems using MRT or EGT outperform the MISO-OFDM system using TR when the modulation order is the same for every subcarrier. The reason for this is mainly due to the fact that MRT and EGT exploit the full spatial diversity equal to N_t, whereas the TR system only exploits half of this diversity order. Furthermore, the EGT system performs very close to the MRT precoding scheme whatever the SNR range and the number of transmit antennas. Nevertheless, the performance loss of the TR scheme is completely compensated with the use of adaptive modulation algorithms. Moreover in this case, we have shown that the TR system is able to achieve a better spectral efficiency for a given SER at low SNRs than the other systems.

Finally, in a MISO-OFDM system, EGT offers a good performance/complexity trade-off when no adaptive modulation is carried out, since it can be applied without any information exchanges between the transmit antennas and with reasonable complexity for the computation of the precoding factor. For systems allowing adaptive modulations, TR turns out to be the best choice with a high number of transmit antennas because it offers the best performance whatever the SNR and it requires the lowest computational complexity of the precoding factors. As an extension to this work, EGT and TR schemes should further be investigated in the context of large MIMO systems as well as for green communications operating at a low-SNR regime [11].

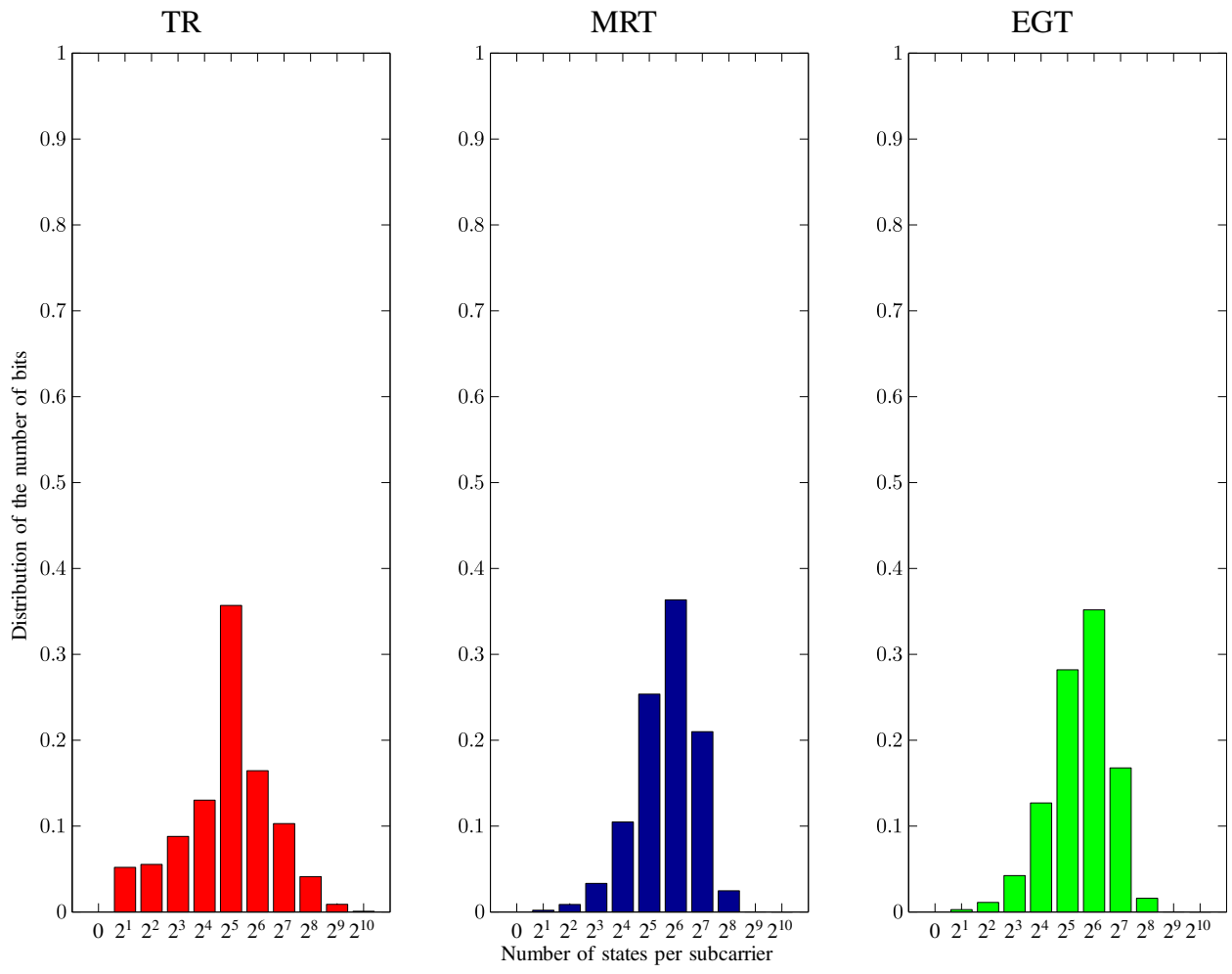

Figure 8 Distribution of number of bits allocated on subcarriers for transmit SNR $\rho = 25$ dB, $N_t = 2$ and target SER of 10^{-5}.

Appendix

Appendix 1: BER of a MISO system using MRT

From Equations 16 and 18

$$\overline{\mathrm{BER}}_{\mathrm{MRT}}(\rho) = \int_0^{+\infty} \frac{1}{\Gamma(N_t)} x^{N_t-1} e^{-x} \frac{1}{2} \mathrm{erfc}\left(\sqrt{x\rho}\right) dx \tag{33}$$

Using the Taylor series of e^{-x}, the formula becomes

$$\overline{\mathrm{BER}}_{\mathrm{MRT}}(\rho) = \frac{1}{2\Gamma(N_t)} \sum_{k=0}^{+\infty} \frac{(-1)^k}{k!} \int_0^{+\infty} x^{k+N_t-1} \mathrm{erfc}\left(\sqrt{x\rho}\right) dx \tag{34}$$

By changing the variables as $z = \sqrt{x\rho}$ and using

$$\int_0^{+\infty} z^{2q-1} \mathrm{erfc}(z) dz = \frac{\Gamma\left(q+\frac{1}{2}\right)}{2\sqrt{\pi} q} \tag{35}$$

with $q = k + N_t$, Equation 34 becomes

$$\overline{\mathrm{BER}}_{\mathrm{MRT}}(\rho) = \frac{1}{\Gamma(N_t)} \sum_{k=0}^{+\infty} \frac{(-1)^k}{k!} \left(\frac{1}{\rho}\right)^{k+N_t} \frac{\Gamma\left(k+N_t+\frac{1}{2}\right)}{2\sqrt{\pi}(k+N_t)} \tag{36}$$

The asymptotic average BER is obtained for high SNR values. The expression of the average BER being a sum of powers of ρ, the limit for high SNR values is the term with the highest power. Hence, the asymptotic BER is equal to the first term of the sum, obtained for $k = 0$:

$$\begin{aligned} \lim_{\rho \to +\infty} \overline{\mathrm{BER}}_{\mathrm{MRT}}(\rho) &= \frac{1}{\Gamma(N_t)} \frac{\Gamma\left(N_t+\frac{1}{2}\right)}{2N_t\sqrt{\pi}} \left(\frac{1}{\rho}\right)^{N_t} \\ &= \frac{1}{(N_t-1)!} \frac{(2N_t)!\sqrt{\pi}}{2^{2N_t}(N_t)!} \frac{1}{2N_t\sqrt{\pi}} \left(\frac{1}{\rho}\right)^{N_t} \\ &= \frac{(2N_t)!}{2^{2N_t+1}(N_t!)^2} \left(\frac{1}{\rho}\right)^{N_t} \end{aligned} \tag{37}$$

Appendix 2: BER of a MISO system using EGT

The case studied is presented in detail in 4.2 where $N_t = 2$. The first step is to compute the PDF of $y = \sum_{k=1}^{2} |H_{m,k}|$. The terms $|H_{m,k}|$ being independent, the PDF of the sum is the convolution of the PDF of each of the term. The modulus $|H_{m,k}|$ following a Rayleigh distribution and knowing that such a distribution is equal to zero for $t < 0$, the PDF can be written as

$$p(y) = \frac{e^{-\frac{y^2}{4\sigma^2}}}{\sigma^4} \int_0^y t(y-t) e^{\frac{-\left(t-\frac{y}{2}\right)^2}{\sigma^2}} dt$$

By changing the variables, one can get to

$$p(y) = \frac{e^{-\frac{y^2}{4\sigma^2}}}{\sigma^3} \int_{-\frac{y}{2\sigma}}^{\frac{y}{2\sigma}} \left(\frac{y^2}{4} - \sigma^2 w^2\right) e^{-w^2} dw$$

Noting that the functions to be integrated are even and performing an integration by parts on the second integral, it becomes

$$p(y) = \frac{e^{-\frac{y^2}{4\sigma^2}}}{\sigma^3} \left\{ \underbrace{\sqrt{\pi} erf\left(\frac{y}{2\sigma}\right)\left(\frac{y^2}{4} - \frac{\sigma^2}{2}\right)}_{T_1} + \underbrace{\frac{y\sigma}{2} e^{-\frac{y^2}{4\sigma^2}}}_{T_2} \right\} \tag{38}$$

Computation of term T_1

Knowing the Taylor series $e^z = \sum_{k=0}^{+\infty} \frac{z^k}{k!}$ and $erf(z) = \frac{2}{\sqrt{\pi}} \sum_{k=0}^{+\infty} \frac{(-1)^k}{k!(2k+1)} z^{2k+1}$, the term T_1 can be developed as

$$\begin{aligned} T_1 =& \frac{e^{-\frac{y^2}{4\sigma^2}}}{\sigma^3} \sqrt{\pi} erf\left(\frac{y}{2\sigma}\right)\left(\frac{y^2}{4} - \frac{\sigma^2}{2}\right) \\ =& \frac{1}{2\sigma^3} \sum_{k=0}^{+\infty} \sum_{l=0}^{+\infty} \frac{(-1)^{k+l}}{k!\, l!\, (2l+1) 2^{2k+2l+1} \sigma^{2k+2l+1}} \\ & \times \left(y^{2k+2l+3} - 2\sigma^2 y^{2k+2l+1}\right) \end{aligned}$$

Integrating T_1 gives the first term of the average BER:

$$\begin{aligned} I_1 =& \int_{-\infty}^{+\infty} T_1 . \frac{1}{2} \mathrm{erfc}\left(y\sqrt{\frac{\rho}{N_t}}\right) dy \\ =& \frac{1}{4\sigma^3} \sum_{k=0}^{+\infty} \sum_{l=0}^{+\infty} \frac{(-1)^{k+l}}{k!\, l!\, (2l+1) 2^{2k+2l+1} \sigma^{2k+2l+1}} \\ & \times \left\{ \int_0^{+\infty} y^{2k+2l+3} \mathrm{erfc}\left(y\sqrt{\frac{\rho}{2}}\right) dy \right. \\ & \left. - 2\sigma^2 \int_0^{+\infty} y^{2k+2l+1} \mathrm{erfc}\left(y\sqrt{\frac{\rho}{2}}\right) dy \right\} \end{aligned}$$

After changing the variables and using Equation 35, I_1 becomes

$$\begin{aligned} I_1 =& \frac{1}{4\sigma^3} \sum_{k=0}^{+\infty} \sum_{l=0}^{+\infty} \frac{(-1)^{k+l}}{k!\, l!\, (2l+1) 2^{2k+2l+1} \sigma^{2k+2l+1}} \\ & \times \left\{ \left(\frac{2}{\rho}\right)^{k+l+2} \frac{\Gamma\left(k+l+\frac{5}{2}\right)}{2\sqrt{\pi}(k+l+2)} \right. \\ & \left. - 2\sigma^2 \left(\frac{2}{\rho}\right)^{k+l+1} \frac{\Gamma\left(k+l+\frac{3}{2}\right)}{2\sqrt{\pi}(k+l+1)} \right\} \end{aligned}$$

By calculating the first terms of I_1, I_{11}, and I_{12} resp., for $k = 0, l = 0$ and $k = 1, l = 0 + k = 0, l = 1$, the terms with the lowest powers of $\frac{1}{\rho}$ are computed, giving the asymptotic BER for T_1:

$$I_{11} = \frac{3}{2^5 \sigma^4} \frac{1}{\rho^2} - \frac{1}{8\sigma^2} \frac{1}{\rho} \tag{39}$$

$$I_{12} = \frac{1}{16\sigma^4} \frac{1}{\rho^2} \tag{40}$$

Computation of term T_2

Integrating T_2 gives the second term of the average BER:

$$\begin{aligned} I_2 =& \int_{-\infty}^{+\infty} T_2 . \frac{1}{2} \mathrm{erfc}\left(y\sqrt{\frac{\rho}{N_t}}\right) dy \\ =& \frac{1}{4\sigma^2} \sum_{k=0}^{+\infty} \frac{(-1)^k}{k!\, 2^k \sigma^{2k}} \int_0^{+\infty} y^{2k+1} \mathrm{erfc}\left(y\sqrt{\frac{\rho}{2}}\right) dy \end{aligned}$$

Changing the variables and using Equation 35, I_2 becomes

$$I_2 = \frac{1}{4\sigma^2} \sum_{k=0}^{+\infty} \frac{(-1)^k}{k!\, 2^k \sigma^{2k}} \left(\frac{2}{\rho}\right)^{k+1} \frac{\Gamma\left(k+\frac{3}{2}\right)}{2\sqrt{\pi}(k+1)}$$

The first terms I_{21} and I_{22} can be computed for $k = 0$ and $k = 1$ resp.:

$$I_{21} = \frac{1}{4\sigma^2} \frac{\Gamma\left(\frac{3}{2}\right)}{2\sqrt{\pi}} \frac{2}{\rho} = \frac{1}{8\sigma^2 \rho} \tag{41}$$

$$I_{22} = \frac{1}{4\sigma^2} \frac{-1}{2\sigma^2} \frac{\Gamma\left(\frac{5}{2}\right)}{2\sqrt{\pi} 2} \frac{2^2}{\rho^2} = -\frac{3}{2^5 \sigma^4} \frac{1}{\rho^2} \tag{42}$$

BER computation

$$\begin{aligned} \lim_{\rho \to +\infty} \overline{\mathrm{BER}}_{\mathrm{EGT}} =& I_{11} + I_{12} + I_{21} + I_{22} \\ =& \frac{1}{16\sigma^4} \frac{1}{\rho^2} \end{aligned} \tag{43}$$

Appendix 3: BER of a MISO system using TR

The computation of the average BER for a MISO-OFDM system using TR as described in Section 2.3 is detailed here. As said in Section 4, the average BER is equal to

$$\overline{\mathrm{BER}}_{\mathrm{TR}}(\rho) = \int_{-\infty}^{+\infty} p(x) . \frac{1}{2} \mathrm{erfc}\left(x\sqrt{\frac{\rho}{N_t}}\right) dx \tag{44}$$

With $p(x)$ given in Equation 18 and using the Taylor series of e^{-x}, the formula becomes

$$\overline{\mathrm{BER}}_{\mathrm{TR}}(\rho)=\frac{1}{2\Gamma(N_t)}\sum_{k=0}^{+\infty}\frac{(-1)^k}{k!}\int_0^{+\infty}x^{k+N_t-1}\mathrm{erfc}\left(x\sqrt{\frac{\rho}{N_t}}\right)dx$$

By changing the variables as $w=x\sqrt{\frac{\rho}{N_t}}$, the BER becomes

$$\overline{\mathrm{BER}}_{\mathrm{TR}}(\rho)=\frac{1}{2\Gamma(N_t)}\sum_{k=0}^{+\infty}\frac{(-1)^k}{k!}\left(\sqrt{\frac{N_t}{\rho}}\right)^{k+N_t}\int_0^{+\infty}w^{k+N_t-1}\times\mathrm{erfc}(w)dw$$

Applying Equation 35 with $q=\frac{k}{2}+\frac{N_t}{2}$, one gets

$$\overline{\mathrm{BER}}_{\mathrm{TR}}(\rho)=\frac{1}{2\Gamma(N_t)}\sum_{k=0}^{+\infty}\frac{(-1)^k}{k!}\frac{\Gamma\left(\frac{k}{2}+\frac{N_t}{2}+\frac{1}{2}\right)}{2\sqrt{\pi}\left(\frac{k}{2}+\frac{N_t}{2}\right)}\left(\sqrt{\frac{N_t}{\rho}}\right)^{k+N_t}\quad(45)$$

Competing interests
The authors declare that they have no competing interests.

Acknowledgements
This work has been sponsored by Agence Nationale de la Recherche (ANR) project 'TRIMARAN'.

Author details
[1]Institute of Electronics and Telecommunications of Rennes (IETR), Rennes 35708, France. [2]Thales Communications and Security, Genevilliers 92230, France.

Received: 4 March 2013 Accepted: 23 October 2013
Published: 9 November 2013

References

1. GJ Foschini, Layered space-time architecture for wireless communication in a fading environment when using multi-element antennas. Bell Labs Tech. J. **1**(2), 41–59 (1996)
2. S Zhou, GB Giannakis, Optimal transmitter eigen-beamforming and space-time block coding based on channel mean feedback. IEEE Trans. Signal Process. **50**(10), 2599–2613 (2002)
3. TKY L o, Maximum ratio transmission. IEEE Int. Conf. Commun. **2**, 1310–1314 (1999)
4. DJ Love, JRW Heath, Equal gain transmission in multiple-input multiple-output wireless systems. IEEE Trans. Commun. **51**(7), 1102–1110 (2003)
5. L Zheng, DNC Tse, Diversity and multiplexing: a fundamental tradeoff in multiple-antenna channels. IEEE Trans. Inf. Theory **49**(5), 1073–1096 (2003)
6. A Paulraj, R Nabar, D Gore, *Introduction to Space-Time Wireless Communications* (Cambridge University Press, NY USA, 2008), pp. 95–96
7. M Fink, Time reversal of ultrasonic fields - part i basic principles. IEEE Trans. Ultrason., Ferroelectr. Freq. Control. **39**(5), 555–566 (1992)
8. G Lerosey, J De Rosny, A Tourin, A Derode, G Montaldo, M Fink, Time reversal of electromagnetic waves. Phys. Rev. Lett. **92**(19), 193904 (2004)
9. P Kyritsi, G Papanicolaou, P Eggers, A Oprea, MISO time reversal and delay-spread compression for FWA channels at 5 GHz. IEEE Antennas Wireless Propagation Lett. **3**(1), 96–99 (2004)
10. A Khaleghi, G El Zein, IH Naqvi, Demonstration of time-reversal in indoor ultra-wideband communication time domain measurement. 4th Int. Symp. Wireless Commun. Syst. **1**, 465–468 (2007)
11. B Wang, Y Wu, F Han, YH Yang, KJR Liu, Green wireless communications: a time-reversal paradigm. IEEE J. Selec. Areas Commun. **29**(8), 1698–1710 (2011)
12. C Oestges, AD Kim, G Papanicolaou, AJ Paulraj, Characterization of space-time focusing in time-reversed random fields. IEEE Trans. Antennas Propagation **53**(1), 283–293 (2005)
13. SQ Xiao, J Chen, BZ Wang, XF Liu, A numerical study on time-reversal electromagnetic wave for indoor ultra-wideband signal transmission. Prog. Electromagnetics Res. **77**, 329–342 (2007)
14. I Naqvi, A Khaleghi, G El Zein, Time reversal UWB communication system: a novel modulation scheme with experimental validation. EURASIP J. Wireless Commun. Network. **2010**, 398401 (2010)
15. D Abbasi-Moghadam, V Vakili, A SIMO one-bit time reversal for UWB communication systems. EURASIP J. Wireless Commun. Network. **2012**(1), 113 (2012)
16. M Emami, M Vu, J Hansen, AJ Paulraj, G Papanicolaou, Matched filtering with rate back-off for low complexity communications in very large delay spread channels. Conf. Rec. Thirty-Eighth Asilomar Conf. Signals, Syst. Comput. **1**, 218–222 (2004)
17. T Dubois, M Hélard, M Crussière, On the use of time reversal for digital communications with non-impulsive waveforms, in *International Conference on Signal Processing and Communication Systems*, (Gold Coast, Dec 2010), pp. 1–6
18. T Dubois, M Hélard, M Crussière, Time reversal in a MISO OFDM system: guard interval design, dimensioning and synchronisation spects. Wireless World Res. Forum. **29**, 1–6 (2012)
19. Y Wang, J Coon, Full rate orthogonal space-time block coding in OFDM transmission using time reversal, in *Proceedings of the IEEE Wireless Communications and Networking Conference*, (Budapest, Apr 2009), pp. 1–6
20. GL Stuber, JR Barry, SW McLaughlin, Y Li, MA Ingram, TG Pratt, Broadband MIMO-OFDM wireless communications. Proc. IEEE **92**(2), 271–294 (2004)
21. JM Cioffi, A multicarrier primer. Report, ANSI T1E1.4/91-157, Committee contribution (1991)

doi:10.1186/1687-1499-2013-260
Cite this article as: Dubois *et al.*: **Performance of time reversal precoding technique for MISO-OFDM systems.** *EURASIP Journal on Wireless Communications and Networking* 2013 **2013**:260.